An Improved Algorithm for Transient Statistical Energy Analysis

Jiang Xu, Jun Guo and Xiaojun Zhao

College of Shipbuilding Engineering, Harbin Engineering University, Harbin 150001, China.
E-mail: paper_gj@163.com

(Received 29 August 2025; accepted 02 November 2025)

The transient statistical energy analysis (TSEA) method is suitable for solving high-frequency structural dynamic response problems, and has been widely used in aerospace and marine fields. However, for complex structures such as hull shells and multi-compartment submersibles, there are problems such as a cumbersome computational process and huge computational volume. This paper proposes the Iterative TSEA (ITSEA) method, which utilizes an iterative approach to solve the energy balance equation combined with initial conditions. Validation shows that compared to TSEA, the ITSEA algorithm saves 40% of computational parameters and processes, while the relative error of the energy decay curve after 20 iterations is no more than 2.1%. ITSEA offers significant advantages for large-scale shock response calculations for complex structures, and for structures with more than 30 subsystems, the improvement in computational efficiency becomes significant.

1. INTRODUCTION

Predicting the high-frequency impact response of complex structures has been a crucial concern across aerospace, maritime, and automotive fields. The existing impact response methods are mostly limited to medium and low frequencies.[1–7] For large and complex structures, it is difficult to solve the high-frequency structural response by purely relying on the kinetic method. The finite element method can predict structural impact responses, but for intricate geometries, it is often constrained by mesh size, leading to convergence issues and excessive computational time. In the last century, the Statistical Energy Analysis (SEA) method was proposed.[8] The SEA method is suitable for solving high-frequency structural dynamics problems under steady state excitation,[9] and later developed into the Transient-SEA (TSEA) method, which extends the scope of application to high-frequency structural dynamics problems under transient excitation as well as widely used in the fields of aerospace, vehicles, and ships.[10] Lyon[11] used the statistical energy analysis method with considerable success to analyze the stationary vibrations of complex systems. Manning and Lee's[12] formulation has been employed with considerable success[13,14] to calculate the decay of vibrations in complex systems after removal of a steady-state excitation. Based on the TSEA method, Mao[15] proposed a set of load identification theories based on the TSEA method, and experimentally verified the identification method through the impact load identification of a double-coupled system. Song[16] established a two-substructure coupling model and investigated how parameter errors affect the substructure response energy in TSEA using a difference method, deriving a relationship function between parameter and energy errors. Sui[17,18] made further improvements to the TSEA method and proposed the Transient Local Energy Approach (TLEA) method to improve the prediction accuracy of the high-frequency shock response, and verified the theory by double-coupled system shock tests. Langley et al[19] derived the TSEA equation in a new way by employing an analogy of the Priestley description of a non-stationary random process. He also applied a number of the concepts of statistical mechanics to structural dynamic systems in order to provide new insights into the system behavior under various conditions.[20] Tso et al.[21] investigated the parameters of the coupling factors in the TSEA method by means of travelling wave analysis for a plate with periodic reinforcement coupled at right angles to a homogeneous slab. Robinson et al.[22] concerns the use of TSEA to predict impact sounds in heavyweight buildings in terms of the maximum fast time-weighted sound pressure level using transient sources of mechanical excitation that have complex force time-histories. Hirakawa[23] extends previous work using TSEA in heavyweight buildings by introducing an inverse form of TSEA to determine the transient structure-borne sound power input from heavy impact sources into a heavyweight base floor with a floating floor. Hopkins[24] used transient and steady-state statistical energy analysis to investigate how the errors depend upon the building structure to which the coupled reception plate is connected. Chen et al.[25] derived the energy governing equations by considering time-varying SEA parameters and energy flow items caused by time-varying damping loss factor, and first applied the SEA method to predict transient energy response of time-varying systems. The spherical impact factor theory proposed by Guo provides a load input calculation method for the TSEA theory.[27] Gong[28,29] used the boundary-element method (BEM) to simulate the physical process of the explosion bubble growth, contraction and collapse while the finite element method (FEM) is used to calculate the glass–epoxy composite structure response to the high pressure induced by the underwater explosion bubble, and used coupled BEM–FEM to handle the interaction of the composite structures and the underwater explosion bubble. Sykora[30] developed Step Matrix Multiplication PI (SMM-PI) method to compute the stochastic response of nonlinear stochastic systems. In addition, numerical tools are generally nice options, including the generalized cell mapping method, path integral approach, Monte Carlo[31–34] simulation and the finite element scheme. Pinnington[35] compared the exact transient energy response of a two-degree-of-

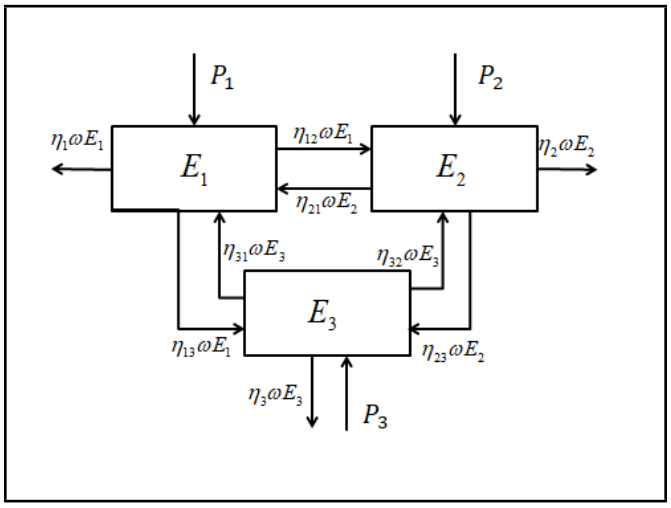

Figure 1. S.E.A. model for a three-oscillator system.

freedom system subject to an impulse from a TSEA on a two coupled system. It is found that the integral of transmitted energy is identical for both approaches.

However, TSEA involves more parameters, leading to cumbersome solution processes and immense computational loads for complex structures, hindering practical applications. For ships, its main structure is a complex system consisting of the main hull, deck, and internal compartments, which contains dozens of subsystems and is difficult to get the high-frequency impact response prediction of the whole hull using the TSEA method. To address this, the proposed method improves TSEA and solving iteratively using initial value conditions, which simplifies computational parameters and processes while enhancing efficiency for intricate systems. In addition, the ITSEA method is used to improve the literature[27] arithmetic example and compare it with respect to computational efficiency and computational time.

2. TRADITONAL TSEA METHOD FOR SOLVING SUBSYSTEM ENERGY EQUATIONS

A transient input is applied to a multi-coupled system, denoted by $E_i(t)$ as the energy of subsystem i at time t. The inputs are expressed as energy in the form of $E_1(0)$, $E_2(0)$ and $E_3(0)$ respectively. The statistical energy model of the system is shown in Fig. 1. In Fig. 1, η_i denotes the internal loss factor of subsystem i, and η_{ij} denotes the coupling loss factor between subsystem i-th and j-th.

The system energy balance equation is shown in Eq. (1):[36]

$$P_{in,i}(\omega,t) = \frac{\partial E_i(\omega,t)}{\partial t} + LF(\omega)\,E(\omega,t); \tag{1}$$

where $P_{in,i}$ denotes the input power of the subsystem, E denotes the subsystem energy, the subscript denotes the subsystem number, LF denotes the time-invariant system loss factor matrix, and w denotes the center frequency of the analyzed band. The differential symbol D is introduced so that $D = d/dt$. For the singular solution, the system determinant is 0 with:

$$\begin{vmatrix} D+\eta_{a1}\omega & -\eta_{21}\omega & \cdots & -\eta_{n1}\omega \\ -\eta_{12}\omega & D+\eta_{a2}\omega & \cdots & -\eta_{n2}\omega \\ \vdots & \vdots & \ddots & \vdots \\ -\eta_{1n}\omega & -\eta_{2n}\omega & \cdots & D+\eta_{an}\omega \end{vmatrix} = 0. \tag{2}$$

The resulting Ds are all real, which means that there is no vibration term in the energy equation. Thus, the energy equation for i-th subsystem can be written as:

$$E_i(t) = \sum_{j=1}^{n} A_{ij} e^{D_j t}, \quad i = 1, 2, \ldots, n; \tag{3}$$

where A_{ij} is the coefficient to be solved. The following is the solution for A_{ij}.

According to Eq. (3), at the initial moment, there is $E_i(0) = \sum_{j=1}^{n} A_{ij}$, where $E_i(0)$ denotes the initial energy of subsystem i. The system's energy input can be obtained from the literature estimation.[27]

For ease of analysis, E_i denotes the energy time history response of subsystem i. Let $P = 0$ in Eq. (1), and at the initial moment, differentiate Eq. 3 and bring it into Eq. (1) to obtain:

$$\frac{dE_i}{dt} = \sum_{j=1}^{n} A_{ij} D_j = -\eta_{ai}\omega E_i - \sum_{\substack{j=1 \\ j\neq i}}^{n} \eta_{ji}\omega E_j; \tag{4}$$

Continuing to do successive $(n-1)$-order differentiation of Eq. 4, we can obtain conditional equations about n^2 mutually independent conditional equations about A_{ij}. and then realize the solution of the coefficients A_{ij} in Eq. (3) to obtain the energy equations of each subsystem.

3. ITSEA METHOD FOR SOLVING SUBSYSTEM ENERGY EQUATIONS

3.1. Example Solution for a Two Subsystem TSEA Model

For double-coupled subsystems, according to Eqs. (2)–(4), there are:

$$D_1, D_2 = -\omega(a \mp b); \tag{5}$$

where $a = (\eta_a + \eta_b)/2$, $b = \sqrt{(\eta_a - \eta_b)^2 + 4\eta_{12}\eta_{21}}/2$, $\eta_a = \eta_1 + \eta_{12}$, $\eta_b = \eta_2 + \eta_{21}$.

The subsystem energy equation is:

$$\begin{aligned} E_1 = {} & \frac{e^{D_1 t}}{2b}\left[\left(-\frac{D_2}{\omega} - \eta_{12}\right)E_1 + \eta_{12}E_2\right] + \\ & \frac{e^{D_2 t}}{2b}\left[\left(\frac{D_1}{\omega} + \eta_{12}\right)E_1 - \eta_{12}E_2\right]; \\ E_2 = {} & \frac{e^{D_1 t}}{2b}\left[\left(-\frac{D_2}{\omega} - \eta_{21}\right)E_2 + \eta_{21}E_1\right] + \\ & \frac{e^{D_2 t}}{2b}\left[\left(\frac{D_1}{\omega} + \eta_{21}\right)E_2 - \eta_{21}E_1\right]; \end{aligned} \tag{6}$$

with $\eta_1 = 0.15$, $\eta_2 = 0.05$, $\eta_{21} = 0.01$, $\omega = 100$. When $E_1(0) = 100$, $E_2(0) = 0$, the energy curve of the dual-oscillator system is shown in the Fig. 2. When $n = 3$, Eq. (2)

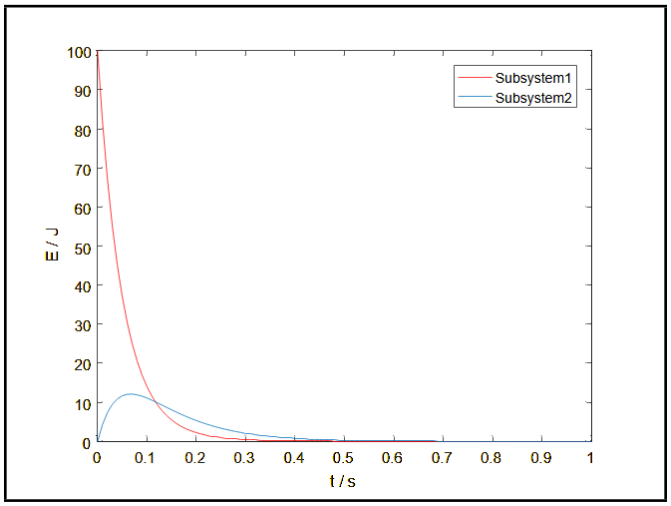

Figure 2. Energy profile of a two-vibrator system.

can be written as:

$$D^3 + \omega D^2 + a\omega^2 D + a^3 C = 0; \tag{7}$$

where

$$A = \sum_{i=1}^{3} \eta_{ai};$$

$$B = \frac{1}{2}\sum_{j=1}^{3}\sum_{\substack{k=1\\k\neq j}}^{3}\left(\eta_{aj}\eta_{ak} - \eta_{jk}\eta_{kj}\right);$$

$$C = -\sum_{i=1}^{3}\sum_{j=1}^{3}\sum_{\substack{k=1\\i\neq j,\, j\neq k,\, i\neq k}}^{3}\left(\frac{1}{2}\eta_{ij}\eta_{ji}\eta_{ak} + \frac{1}{3}\eta_{ij}\eta_{jk}\eta_{ki} + \frac{1}{6}\eta_{ai}\eta_{aj}\eta_{ak}\right).$$

The solution of Eq. (7) can be written in the following form: $D_1 = \omega a_a$, $D_2 = \omega b_b$, $D_3 = \omega c_c$, where $a_a + b_b + c_c = -A$; $a_a b_b + b_b c_c + a_a c_c = B$; $a_a b_b c_c = -C$.

The subsystem energy equation is:

$$E_{pi} = \omega^2\left[\left(\frac{D_p D_q}{\omega^2} + \left(\eta_{ai}+\frac{D_p}{\omega}\right)\left(\eta_{ai}+\frac{D_q}{\omega}\right) + \eta_{ij}\eta_{ji} + \eta_{ik}\eta_{ki}\right)E_i(0) + \left(\eta_{jk}\eta_{ki} - (\eta_{ai}+\eta_{aj})\eta_{ji} - \frac{D_p+D_q}{\omega}\eta_{ji}\right)E_j(0) + \left(\eta_{kj}\eta_{ji} - (\eta_{ai}+\eta_{ak})\eta_{ki} - \frac{D_p+D_q}{\omega}\eta_{ki}\right)E_k(0)\right] \Big/ \left((D_r-D_p)(D_r-D_q)\right); \tag{8}$$

where $i, j, k \in [1,3]$, $p, q, r \in [1,3]$ and $i \neq j \neq k, p \neq q \neq r$.

When n continues to increase, the solution process of Eq. 3 becomes more complicated and the coefficient terms become more cumbersome, which inconveniences the work of solving the energy equation for calculation and theoretical analysis of energy curves. Furthermore, the increase in the number of subsystems has also reduced computational and analytical efficiency, while complicating the formulation of results in mathematical expressions.

3.2. Improvements To The TSEA Methodology—ITSEA

3.2.1. Energy Decay Rate Analysis

As can be seen by the energy profile of the two-oscillator system in Fig. 2, the energy decay rate of the damped system is fast, and when $E_2(0) = 0$, Eq. (6) becomes:

$$E_1 = \frac{E_0}{2b}e^{-a\omega t}\left[\left(\frac{-D_2}{\omega} - \eta_a\right)e^{b\omega t} + \left(\frac{D_1}{\omega} + \eta_a\right)e^{-b\omega t}\right]; \tag{9}$$

$$E_2 = \frac{E_0}{2b}\eta_{12}e^{-a\omega t}\left(e^{b\omega t} - e^{-b\omega t}\right).$$

Differentiating Eq. (9) and making it zero yields the moment corresponding to the peak of subsystem 2:

$$t_2 = \frac{\ln\frac{a+b}{a-b}}{2b\omega}. \tag{10}$$

Equation (10) is solved using the data given in Section 3.1. It is calculated that $t_2 = 0.0669$ s, at which point the subsystem 1 energy value has decayed to 26.6%. This indicates that the energy of the damped system changes very fast, and from Eq. (10) it can also be seen that the higher the frequency, the earlier the energy peak appears, the faster the energy decay.

3.2.2. ITSEA Methodology

To simplify the energy equation's calculation, a Taylor expansion of Eq. (3) is performed, since the energy rise and decay is very rapid with the peak close to $t = 0$. Therefore, the energy curve obtained by doing the Taylor expansion of the energy equation (i.e., the McLaughlin expansion) now of $t = 0$ can be controlled in a very small range of error. The McLaughlin expansion of Eq. (3) is as follows:

$$E_i(t) = E_i(0) + tE_i'(0) + \frac{t^2}{2!}E_i''(0) + \cdots + \frac{t^n}{n!}E_i^{(n)}(0) + R_n(t); \tag{11}$$

Its stage error is:

$$\mathbb{R}_n(t) = \frac{E^{(n+1)}(\theta t)}{(n+1)!}t^{n+1}, \qquad 0 < \theta < 1. \tag{12}$$

We can get from Eq. (12) that the larger the order n or the smaller the time t, the smaller the error of the expansion equation. We can also get from Eq. (10) that the corresponding moment of the curve's peak is related to the analyzed frequency band, and the higher the frequency band, the earlier the peak appears, so under the condition of the same number of iterations, the calculation accuracy of the peak of the energy response in the high frequency band will be relatively high. Taking the loss factor parameters set in Section 3.1, assuming that the energy peak appears before 0.1 s, take $t = 0.1$ s $\theta = 1$. After performing 10 iterations of calculation, according to Eq. (12) we can get the stage error $\mathbb{R}(n) = 0,0062$.

Solving for the coefficients $E_i^{(\gamma)}$ and referring to Eq. (4), the continuous n-th order derivative of the function $E_i(t)$ at $t = 0$

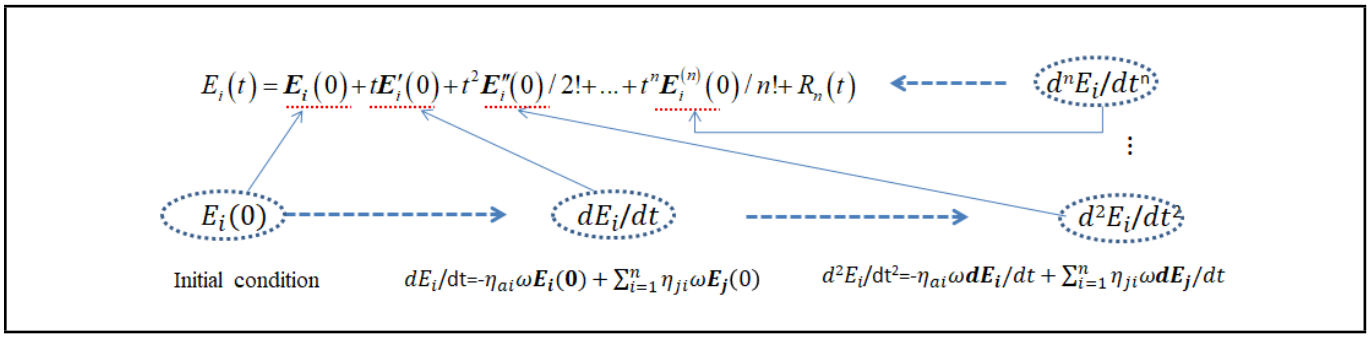

Figure 3. Schematic diagram of the iterative flow of ITSEA.

is:

$$\left.\frac{dE_i}{dt}\right|_{t=0} = -\eta_{ai}\,\omega\,E_i + \sum_{\substack{j=1\\ j\neq i}}^{N}\eta_{ji}\,\omega\,E_j; \tag{13a}$$

$$\left.\frac{d^2E_i}{dt^2}\right|_{t=0} = -\eta_{ai}\,\omega\,\frac{dE_i}{dt} + \sum_{\substack{j=1\\ j\neq i}}^{N}\eta_{ji}\,\omega\,\frac{dE_j}{dt}; \tag{13b}$$

$$\left.\frac{d^{(n)}E_i}{dt^{(n)}}\right|_{t=0} = -\eta_{ai}\,\omega\,\frac{d^{(n-1)}E_i}{dt^{(n-1)}} + \sum_{\substack{j=1\\ j\neq i}}^{N}\eta_{ji}\,\omega\,\frac{d^{(n-1)}E_j}{dt^{(n-1)}}. \tag{13c}$$

In Eq. (13a), $E_i(0)$ is the system input, while η and ω are known parameters, allowing easy calculation of E's first-order derivative at $t = 0$.While the solution of Eq. (13b) takes Eq. (13a) as the conditional input, it can be found by analogy that from (a) to (n), each level of the solution process takes the result of the previous level as the input, so the computational process of Eq. (12) is essentially an iterative process step by step (see Fig. 3).

Iteratively solving Eq. (12) yields the coefficients in subsystem i's energy equation analytically. This simplified formula can eliminate the calculation process of parameter D and coefficient matrix A_{ij}, and only a simple iterative process can realize the solution of the energy equation, so that the calculation process can be greatly reduced. We can see from Fig. 4 that compared to TSEA's 5 steps and parameters, ITSEA reduces these to 3, a 40% saving. ITSEA's iteration number K can be freely adjusted for desired accuracy.

3.3. Solution for the Matrix of Loss Factors

The loss factor is a key parameter in the calculation process, whether it is the ITSEA method or the TSEA method. The loss factor matrix contains internal loss factor (ILF) and coupling loss factor (CLF). For the former, it can be obtained by the transient envelope attenuation method. The basic idea is to obtain the envelope of the acceleration response curve of the subsystem through the Hilbert transform, and then take the logarithm of the envelope, and the ratio of the slope of the logarithmic curve to the frequency ω which is the internal loss factor of the subsystem. The latter needs to be obtained through the energy balance equation.

3.3.1. Transient Envelope Attenuation Method for ILF

Internal Loss Factor is obtained by making Hilbert transform to the acceleration signal from the experiment:[37]

$$\hat{a}(t) = H[a(t)] = a(t) * \frac{1}{\pi t} = -\frac{1}{\pi t}\int_{-\infty}^{+\infty}\frac{a(\tau)}{t-\tau}\,d\tau; \tag{14}$$

where $a(t)$ represents the acceleration response of the structure after impact, and symbol $*$ represents convolution.

The analytic signal of the real function is obtained:

$$u(t) = a(t) + j\hat{a}(t). \tag{15}$$

The plural expressions of $u(t)$ is:

$$u(t) = A(t)e^{j\theta t}; \tag{16}$$

where $A(t) = \sqrt{a(t)^2 + \hat{a}(t)^2}$, A is the envelope of the response signal, and the instantaneous phase $\theta(t)$ is $\arctan(\hat{a}(t)/a(t))$. So, any real function can be represented as $a(t) = A(t)\cos(\theta)$. The attenuation curve can be obtained by taking the envelope of the response signal to the logarithm, and the absolute value of the slope of the curve is $\xi \cdot \omega$, which respectively refers to the damping ratio and the central frequency. Dividing it by the central frequency, it yields the damping ratio ξ.The damping ratio is twice the mean ILF in the measured structural frequency band, i.e., $\eta = 2\xi$.

3.3.2. Energy Balance Equation for CLF

The energy balance equation of the two coupled system can be expressed by Eq. (18):[26]

$$[E_{in,i}]/2\omega = [LF] \times [\varepsilon_{k,i}]; \tag{17}$$

where $E_{in,i}$ is the input energy of the i-th subsystem; ω represents the central frequency of the analysis frequency band; and $e_{k,i}$ represents the average kinetic energy when the i-th subsystem is impacted. $[LF]$ is the matrix of loss factors. Although the energy balance equation represented by Eq. (18) is in the same form as the power flow equilibrium equation under steady state excitation, the effect of excitation on the system is characterized by energy rather than average input power due to the energy limitation of transient excitation.[38]

According to the Parseval energy theorem, the input energy $E_{in,\Delta\omega}$ of the impact load within the analysis frequency band $\Delta\omega$ can be calculated by the following formula:[26]

$$E_{in,\Delta\omega} = \frac{\mathrm{Re}[\langle Y(\omega)\rangle_{\Delta\omega}]}{\pi}\int_{\omega_c-\Delta\omega/2}^{\omega_c+\Delta\omega/2}|F(\omega)|^2\,d\omega. \tag{18}$$

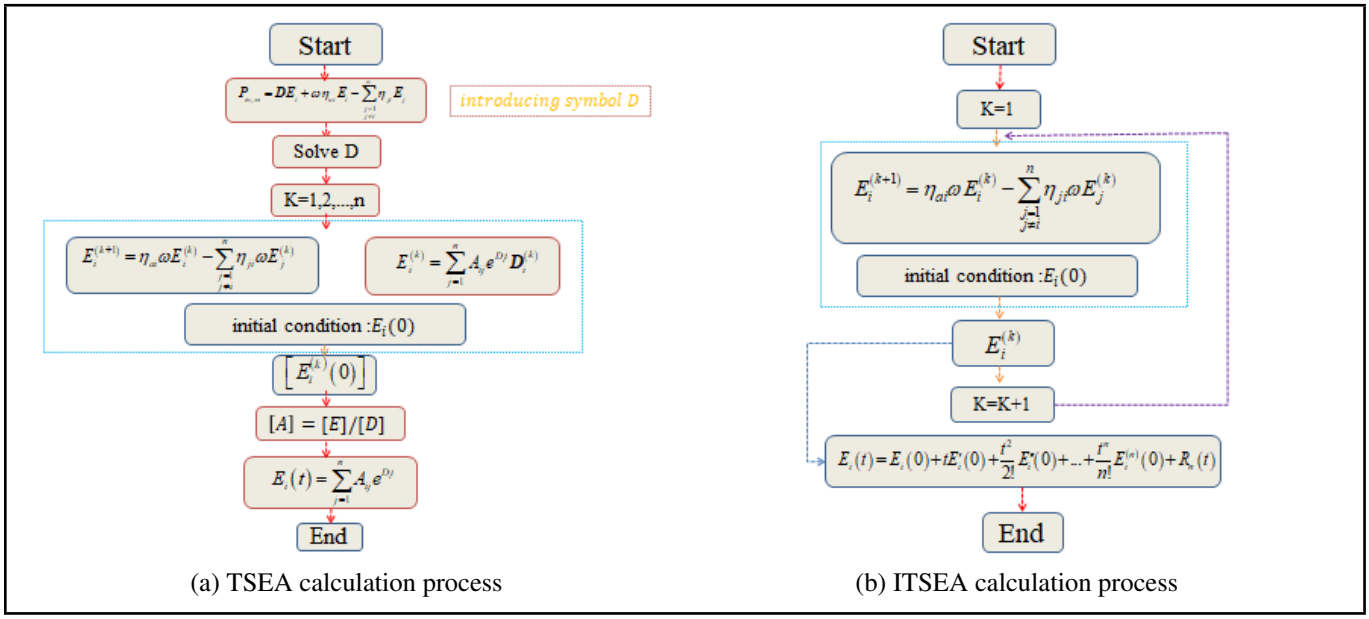

(a) TSEA calculation process (b) ITSEA calculation process

Figure 4. Comparison of calculation process before and after optimization.

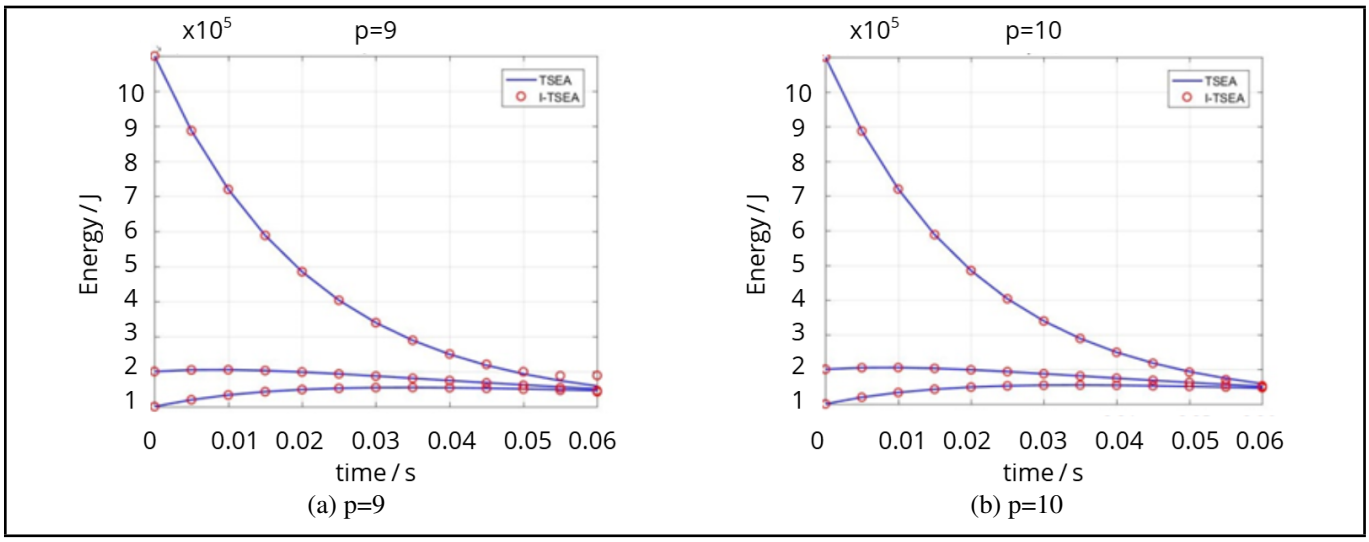

(a) p=9 (b) p=10

Figure 5. Comparison of the peak of energy curve between TSEA method and ITSEA method.

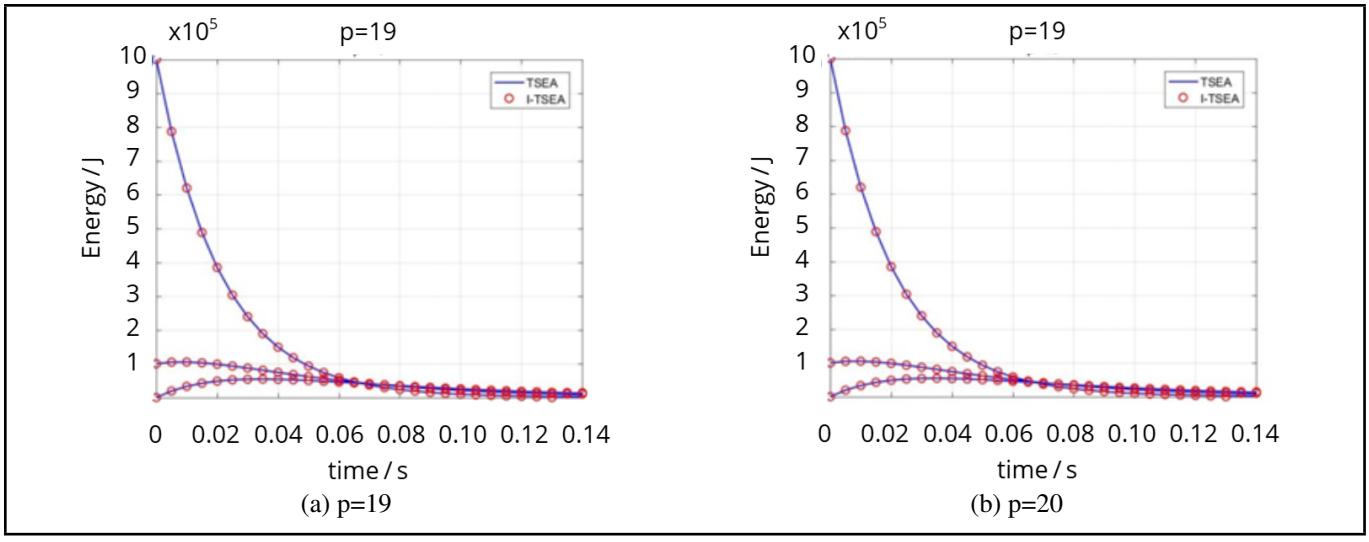

(a) p=19 (b) p=20

Figure 6. Comparison of the energy curve between TSEA method and ITSEA method.

Table 1. Comparison of the results of the two methods for calculating the peak energy value of the subsystem (5 significant figures).

Number of iterations	Subsystem 2 peak energy/10^4J			Subsystem 3 peak energy/10^4J		
	TSEA	ITSEA	relative error	TSEA	ITSEA	relative error
7	10.518	10.518	0	5.4440	5.3922	-0.952%
8	10.518	10.518	0	5.4440	5.4587	0.270%
9	10.518	10.518	0	5.4440	5.4415	-0.045%
10	10.518	10.518	0	5.4440	5.4444	0.007%

Table 2. Calculation error statistics of the ITSEA method energy profile.

Number of iterations	Average relative error			Maximum relative error		
	Subsystem 1	Subsystem 2	Subsystem 3	Subsystem 1	Subsystem 2	Subsystem 3
18	0.94%	0.07%	0.04%	21.55%	1.42%	0.75%
19	0.25%	0.02%	0.01%	6.09%	0.40%	0.20%
20	0.06%	0.01%	0%	1.64%	0.11%	0.06%
21	0.02%	0%	0%	0.42%	0.03%	0.01%

The formula is suitable for all finite plates as well as infinite plates, where $|Y(\omega)|_{\Delta\omega}$ is the average velocity admittance. In the upper formula: $E_{in,\Delta\omega}$ represents the input energy of the impact load in the analysis frequency band $\Delta\omega$; ω_c is the central frequency of the analysis frequency band; ρ_s is the surface mass density of the plate; R is the bending turning radius of the plate (which $R = \sqrt{I/S}$; I is the flat section of the inertial moment of the neutral axis; S is the finite plate cross section area); C_1 is the longitudinal wave velocity, and $C_1 = 5500$ m/s for a steel plate.

The average kinetic energy of the i-th subsystem in the frequency band can be obtained from the following formula according to the Parseval Theorem:

$$\varepsilon_{k,i} = \frac{M_i}{2\pi} \left\langle \int_{\omega_c-\Delta\omega/2}^{\omega_c+\Delta\omega/2} |V_i(\omega)|^2 \, d\omega \right\rangle_s ; \qquad (19)$$

where: M_i is the total mass of the i-th subsystem, and symbol $\langle\cdot\rangle_s$ represents the space average. The frequency segmentation in data analysis in this paper adopts one-third octave bands.

3.4. Advantages of ITSEA

3.4.1. Calculation Accuracy Analysis

In general, damped systems have internal loss factors around $10^{-3} \sim 10^{-1}$ and the coupling loss factors around $10^{-5} \sim 10^{-2}$, decreasing with frequency.[26] To check the calculation accuracy of the ITSEA method, a common simple three-subsystem coupling structure is selected to carry out the energy response calculation. We take $\eta_1 = 0.04$, $\eta_2 = \eta_3 = 0.02$, $\eta_{12} = \eta_{13} = 0.004$, $\eta_{21} = \eta_{31} = 0.001$, $\eta_{23} = 0.005$, $\eta_{32} = 0.001$, $\omega = 100$, and set the inputs to $E_1 = 10^6$ J, $E_2 = 10^5$ J, $E_3 = 10^4$ J.

The efficiency of TSEA is partly dependent on the choice of time step for which Robinson and Hopkins[39] discusses suitable time intervals, from which Guasch and Garcia[40] go on to propose local time stepping.

The computational time step determines the data sampling frequency, which in turn affects computational accuracy and efficiency. Since the energy curve length range of interest in this paper falls within 0.1 s, a time step of 0.001 s was selected for both the TSEA and ITSEA methods. ensuring computational accuracy while maintaining computational efficiency. Since both algorithms compute strides consistently, the comparison of computational efficiency yields more compelling results.

Figures 5 and 6 show the comparison of the calculation results between the TSEA method and the ITSEA method.

In Figs. 5 and 6, p denotes the number of iterations, the number of coefficient terms retained in Eq. (11). The above images demonstrate that after 10 iterations, the ITSEA method can accurately predict the energy curve prior to the response peak; after 20 iterations, the ITSEA method can reasonably accurately predict the entire energy curve before the end of decay. The relative computational errors are shown in Table 1.

To compare the full energy decay curves of the two methods, calculations between $0 - 0.14$ s (when the energy decays to 0.14 s, the subsystem's energy has diminished to 0.63% of its initial value, further analysis is no longer meaningful) were used to obtain the relative errors (by averaging over this range):

$$\Delta = \frac{\sum_{i=1}^{n} \mathrm{abs}(E_{TSEAi} - E_{I\_TSEAi})/E_{TSEAi}}{n}; \qquad (20)$$

where n is the number of discrete time points. The calculation results are shown in Table 2.

As can be seen from Tables 1 and 2, if we are only concerned about the energy change near the peak value of the energy fluctuation of the subsystem, around 10 iterations yield peak energy errors $< 1\%$; if we need to analyze the whole energy decay process, 20 iterations provide $> 98\%$ accuracy over the full decay compared to traditional TSEA. Testing showed that for internal loss factors around $10^{-3} \sim 10^{-1}$ and coupling factors around $10^{-5} \sim 10^{-2}$, 15 ITSEA iterations satisfy $< 1\%$ peak energy error, while 22 iterations satisfy $< 2\%$ relative error over the full attenuation process.

3.4.2. Computational Efficiency Analysis

From Eq. (4), the number of conditional equations required by the TSEA method in solving the structural response is related to the number of subsystems. If only the peak energy is needed, TSEA requires more conditionals than ITSEA iteration counts when subsystems exceed 10; for the full energy curve, TSEA requires more conditionals than ITSEA iterations when subsystems exceed 20. Thus, TSEA's computational efficiency declines while ITSEA's efficiency advantage becomes pronounced as subsystems increase.

With the increase in the number of subsystems, the advantage of the ITSEA method in computational efficiency will be more obvious. Table 3 compares the computational efficiency of the two methods when solving damped systems with different numbers of subsystems. Table 3 shows that the original method required 6.8 hours for solution when subsystems

Table 3. Comparison of the computational efficiency of the two methods.

Number of subsystems	Time for TSEA / s	Time for ITSEA / s	Ratio	Efficiency Improvement
3	1	1	1.00	0%
8	4	4	1.00	0%
10	5	4	0.80	20.0%
15	7	5	0.71	28.6%
20	12	8	0.67	33.3%
30	68	39	0.57	42.6%
100	5005	927	0.19	81.48%
200	24512	3568	0.15	85.44%

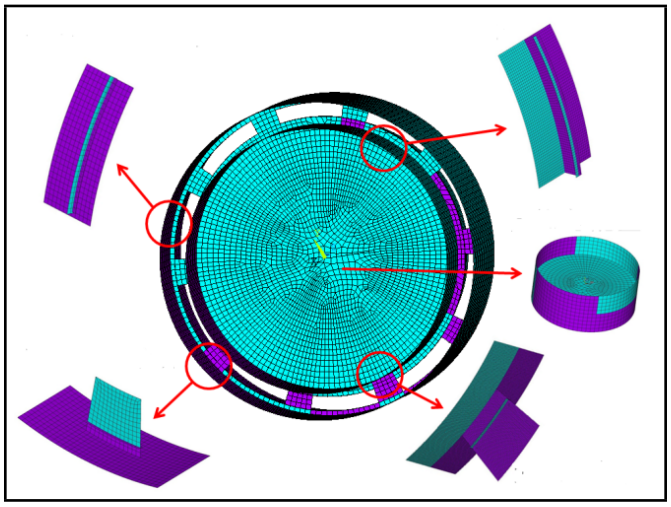

Figure 7. Schematic diagram of the model structure.

reach 200, while the ITSEA method reduced solution time to 0.9 hours — an 85.44% improvement in computational efficiency. The submersible has a complex structure, which may contain hundreds of subsystems, the ITSEA method significantly enhances structural solution efficiency.

Considering hardware influence, case validations across different computer configurations showed ITSEA's computational efficiency improvement rate matching Table 3's data when subsystems exceeded 10.

4. ALGORITHM VALIDATION

4.1. Model Information

TSEA's accuracy for high-frequency impact response has been verified in literature[26] by experiments. This example, which is chosen from the literature,[26] aims to verify the efficiency and accuracy of the ITSEA method. In Section 5.1 of the literature,[26] the cylindrical shell segment model of the ship is used, and the authors divide the entire segment into 131 subsystems, 240 point-coupling boundaries and 160 line-coupling boundaries. The internal structure of the model is shown in Fig. 7.

Applying ITSEA first requires defining subsystems comprised of mode groups able to store vibration energy. Only some similar resonance modes constituting the resonant motion of the subsystem can store energy. At present, the important principle for establishing the subsystem of ITSEA model is that the modal density is high enough, generally with over 5 structural modes in the analyzed frequency band.

Details of the structure dimensions are shown in Table 4 and Figs. 8, 9, and 10.

From the above information, the radius of the cylindrical shell is 1.188 m and thickness t is 0.01 m. Taking the longitudinal wave velocity of steel as $C_1 = 5500$ m/s, the ring frequency of the cylindrical shell $f_r = C_1/2\pi a = 737.2$ Hz, its modal density can be written as in the semi-empirical formula:[17]

Table 4. Plate thickness information for each structure (unit: mm).

t_1	t_2	t_3	t_4
5	5	20	10

$$n(f) = \begin{cases} \dfrac{5A}{\pi h C_1}\left(\dfrac{f}{f_r}\right)^{1/2}, & f/f_r \le 0.48; \\ \dfrac{7.2A}{\pi h C_1}\left(\dfrac{f}{f_r}\right), & 0.48 < f/f_r \le 0.83; \\ \dfrac{2A}{\pi h C_1}\left\{2 + \dfrac{0.596}{F - 1/F}\left[F\cos\left(\dfrac{1.745\, f_r^2}{F^2 f^2}\right) - \dfrac{1}{F}\cos\left(\dfrac{1.745\, F^2 f_r^2}{f^2}\right)\right]\right\}, & f/f_r > 0.83; \end{cases} \tag{21}$$

where A and h are the surface area and thickness of the cylindrical shell, respectively, and F is the bandwidth factor (= [upper frequency/lower frequency]^(1/2)). For one-third octave, the bandwidth factor $F = 1.122$.

After dividing the analyzed bands according to one-third octave, the number of modes in each band is shown in Table 5.

From Table 5, the number of modes in the frequency band above 125 Hz is greater than 5. When approaching the ring frequency, many modes are involved in the resonance, and the modal density of the cylindrical shell reaches the peak currently. At higher frequencies, the shell's curvature-stiffening effect diminishes and modal density approaches that of a flat plate. At this time, the curvature of the cylindrical shell that was brought about by the toughening effect is no longer obvious, so the analysis band was selected as 125 Hz–2500 Hz.

4.2. Results Analysis

To facilitate the analysis, three typical subsystems' energy responses were solved in each frequency band using ITSEA and TESA algorithm, with results compared as follows. In Fig. 11, E_i denotes the energy response curve of the ith subsystem obtained by the TSEA algorithm, and IE_i denotes the response curve obtained by the ITSEA algorithm.

Since the duration of interest does not exceed 0.1 seconds, the analysis time step is set to 0.001 seconds to balance computational accuracy and efficiency.

We can understand from Fig. 11 that the rate of energy decay varies across different subsystems. This is because the differences in the structural characteristics of different subsystems determine their distinct vibration modes, which in turn lead to differences in the frequency response functions and ultimately result in variations in the energy dissipation rates.

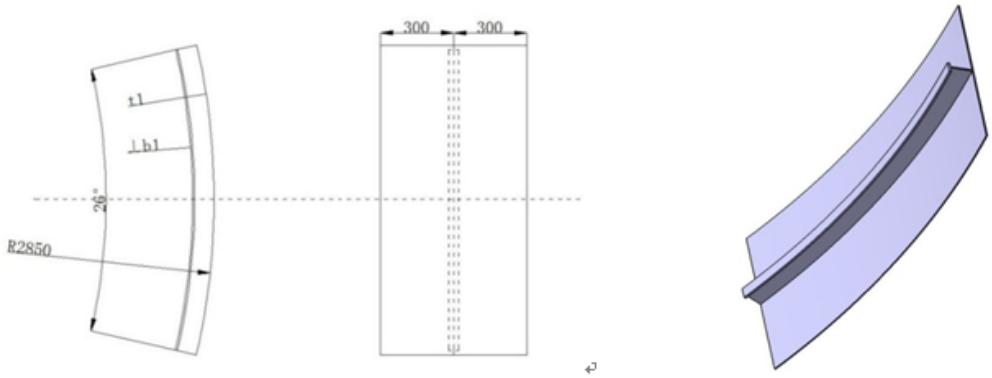

(a) Shell—Internal Reinforcement Coupling system

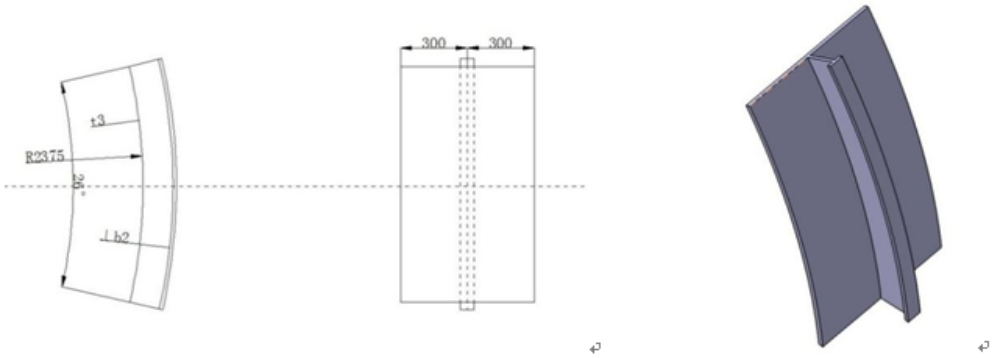

(b) Shell—External Reinforcement Coupling system

Figure 8. Shell—Reinforcement Coupling system.

Table 5. Number of modes in each band.

Frequency Band / Hz	100–125	125–160	160–200	200–250	250–315	315–400	400–500
Modal density	0.17	0.19	0.21	0.24	0.27	0.30	0.38
Mode count	4	6	8	12	17	25	37
Frequency Band / Hz	500–630	630–800	800–1000	1000–1250	1250–1600	1600–2000	2000–2500
Modal density	0.47	0.67	0.61	0.53	0.48	0.46	0.45
Mode count	61	113	121	131	169	184	227

Table 6. Energy Response Relative Error Statistics

Frequency band	Relative error of energy curve		Peak relative error
	Subsystem 1–100	Subsystem 100–131	
125Hz–160Hz	0.58%	0.46%	$< 0.1\%$
160Hz–200Hz	0.55%	0.35%	$< 0.1\%$
200Hz–250Hz	0.21%	0.07%	$< 0.1\%$
250Hz–315Hz	1.71%	0.14%	$< 0.1\%$
315Hz–400Hz	0.95%	0.43%	$< 0.1\%$
400Hz–500Hz	2.07%	0.15%	$< 0.1\%$
500Hz–630Hz	1.35%	0.11%	$< 0.1\%$
630Hz–800Hz	0.90%	0.17%	$< 0.1\%$
800Hz–1000Hz	0.01%	0.01%	$< 0.1\%$
1000Hz–1250Hz	0.11%	0.97%	$< 0.1\%$
1250Hz–1600Hz	0.03%	0.01%	$< 0.1\%$
1600Hz–2000Hz	0.02%	0.01%	$< 0.1\%$
2000Hz–2500Hz	0.56%	0.08%	$< 0.1\%$

According to Eq. (13), the relative errors of the energy response curves and the relative errors of the peak energy values of the subsystems in each analyzed frequency band obtained by using the two algorithms respectively are statistically as shown in Table 6.

In Fig. 11, the solid line shows TSEA results while the dashed line shows nearly coincident ITSEA results. The Eq. (13) is used to calculate the relative error of the two methods, and the maximum relative error of the energy response curves of each subsystem in each frequency band is 2.07%, i.e., over 97% accuracy was maintained.

Table 7. Computational Efficiency Comparison

Number of subsystems	Time / s		
	TSEA	ITSEA	Efficiency improvement rate
10	5	4	20.00%
50	377.62	175.70	53.47%
100	5005.07	926.99	81.48%
131	20548.12	3172.80	84.56%

The computational efficiency of the two algorithms for different number of subsystems respectively is compared in Table 7. Solving the energy equation of the coupled structure of 131 subsystems by the TSEA method takes 20548.1 s in a single time, and the ITSEA method takes 3172.8 s, an 84.56% computational efficiency improvement.

5. CONCLUSIONS

This paper proposed the ITSEA method, an approximate iterative calculation approach using initial value conditions to perform a McLaughlin expansion of traditional TSEA equa-

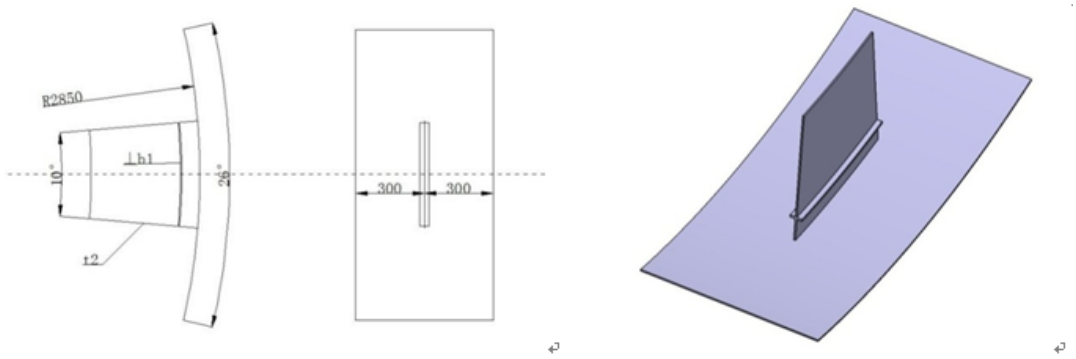

(a) Pallet—Internal Reinforcement Coupling system

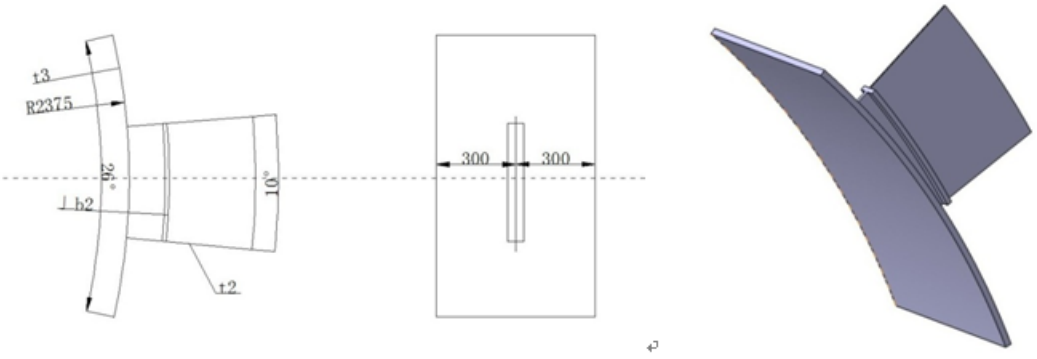

(b) Pallet—External Reinforcement Coupling system

Figure 9. Pallet—Reinforcement Coupling system.

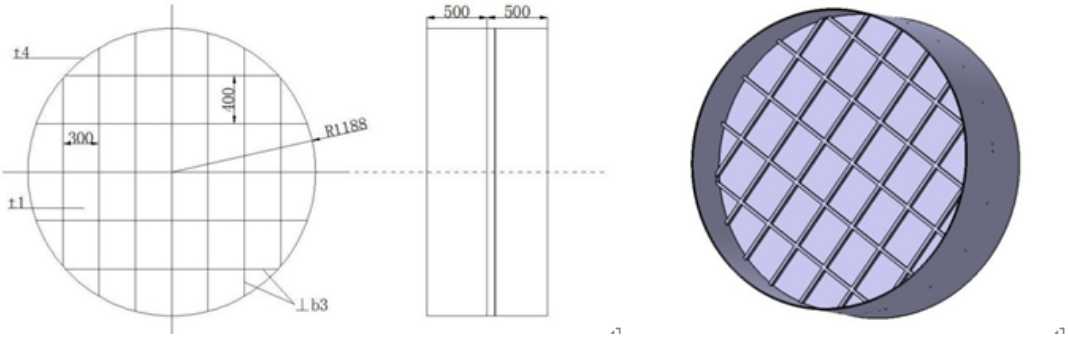

Figure 10. Shell—Bulkhead Coupling system.

tions. The ITSEA method simplified the computational process for impact dynamic response while maintaining computational accuracy. After theoretical derivation and experimental verification, the following conclusions can be drawn:

1. Compared to traditional TSEA, ITSEA saves 40% of computational processes and 40% of parameters, greatly simplifying high-frequency shock response prediction;
2. In terms of calculation accuracy, compared with the TSEA method, ITSEA controls peak energy error within 1% for around 10 iterations. Analyzing the full decay requires about 20 iterations, after which ITSEA's accuracy is over 98% relative to TSEA;
3. ITSEA offers significant advantages for large-scale shock response computation. Its computational efficiency advantage emerges when subsystems exceed 10 and increases with more subsystems. For 131 subsystems, ITSEA maintains over 97% accuracy relative to the original method while improving computational efficiency by 84.56%.

REFERENCES

[1] Qian, J. M., Chen, L. C. and Sun, J. Q., Transient response prediction of randomly excited vibro-impact systems via RBF neural networks, *Journal of Sound and Vibration*, **546**, 117456, (2023). https://doi.org/10.1016/j.jsv.2022.117456

[2] Cui, L. L., Zhang, X. H. and Hao, H., Improved analysis for impact response prediction of reinforced concrete structures considering stress wave propaga-

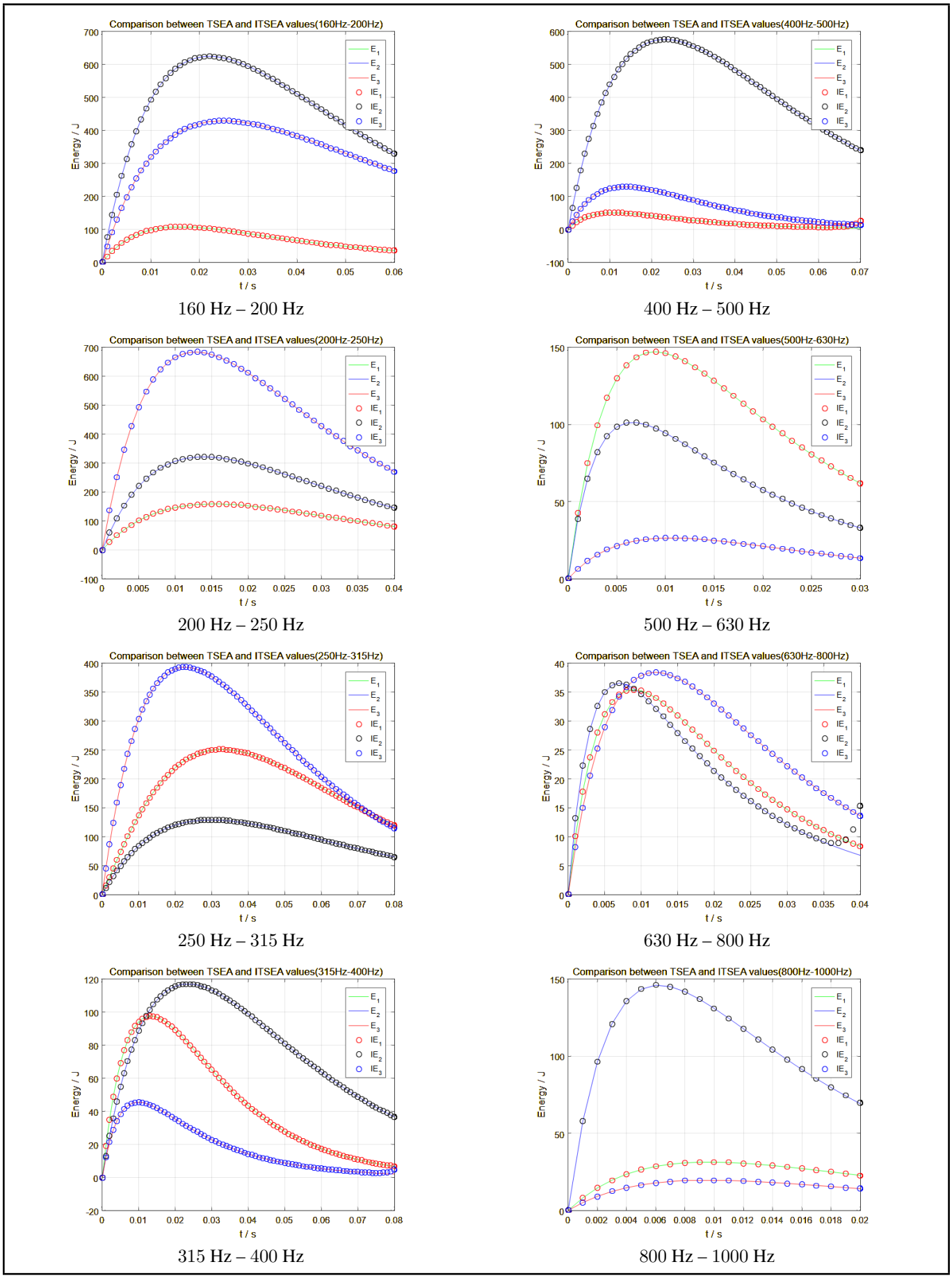

Figure 11. Comparison of the energy curve between TSEA method and ITSEA method.

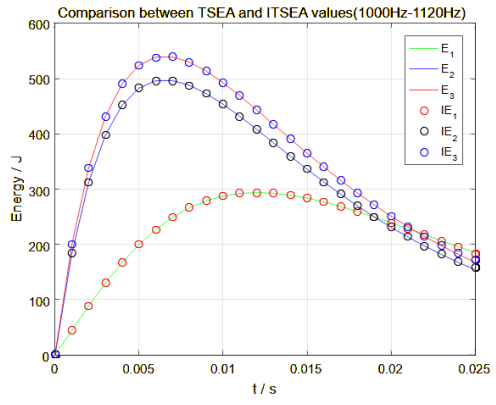

1000 Hz – 1250 Hz

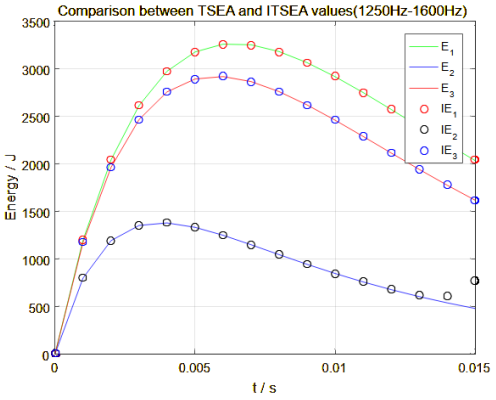

1250 Hz – 1600 Hz

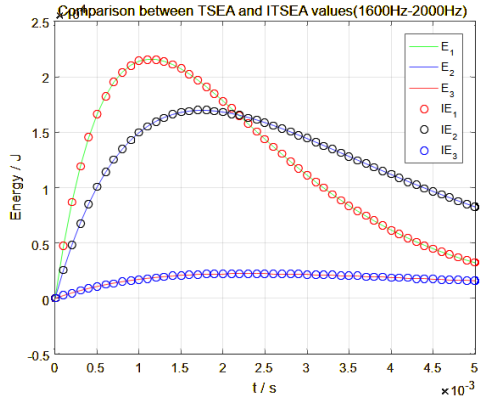

1600 Hz – 2000 Hz

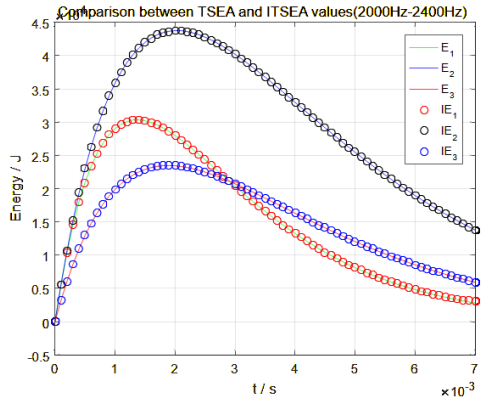

2000 Hz – 2400 Hz

Figure 11-cont. Comparison of the energy curve between TSEA method and ITSEA method.

tion and time dependent shape function, *International Journal of Impact Engineering*, **182**, 104783, (2023). https://doi.org/10.1016/j.ijimpeng.2023.104783

[3] Li, X. W., *Research on impact response characteristics of ship compartment segments based on dynamic substructure method*, Harbin Engineering University, (2018).

[4] Wen, Y. Y., *A hybrid modeling approach for underwater blast impact environmental prediction on ships*, Harbin Engineering University, (2017).

[5] Hawes, D. H., Langley, R. S., Butlin, T. et al., A hybrid finite element–statistical energy analysis method for impulsive and transient loading, *Journal of Sound and Vibration*, **459**, 114849, (2019). https://doi.org/10.1016/j.jsv.2019.114849

[6] Ji, C. Y., Ji, B., Guo, J. T. et al., Numerical prediction for shock response of ship structures based on acoustic structure coupling method, *Journal of Jiangsu University of Science and Technology*, **34**, (2020).

[7] Wagg, J. D. and Chatter, R. S., Sticking and chaotic impacting motion in a two-degree of freedom impact oscillator, *International Journal of Bifurcation and Chaos*, **11**, 57–71, (2001). https://doi.org/10.1142/S0218127401001943

[8] Lai, M. L. and Soom, A., Prediction of transient vibration envelopes using statistical energy analysis techniques, *Journal of Vibration and Acoustics*, **112**, 127–137, (1990). https://doi.org/10.1115/1.2930088

[9] Li, Y. H., Mu, X. H., Pang, F. Z. et al., Experimental validation of underwater radiated noise based on statistical energy method, *Proceedings of Acoustics Symposium in Western China*, 4, (2019).

[10] Langley, R. S., Hawes, D. H., Butlin, T. et al., A derivation of the transient statistical energy analysis equations with benchmark applications to plate systems, *Journal of Sound and Vibration*, **445**, 88–102, (2019). https://doi.org/10.1016/j.jsv.2019.01.002

[11] Lyon, R. H., *Statistical Energy Analysis of Dynamical Systems: Theory and Applications*, MIT Press, Cambridge, MA, (1970).

[12] Manning, J. E. and Lee, K., *Predicting mechanical shock transmission*, *Shock and Vibration Bulletin*, **37**, 65–70, (1968).

[13] Powell, R. E. and Quartararo, L. R., Statistical energy analysis of transient vibration, *ASME Winter Meeting*, Boston, MA, 3–7, (1987).

[14] Sun, H. B., Sun, J. C. and Richards, E. J., Prediction of total loss factors of structures Part III: Effective loss factors in quasi-transient conditions, *Journal of Sound and Vibration*, **106**, 465–479, (1986). https://doi.org/10.1016/0022-460X(86)90192-6

[15] Mao, B. Y., Xie, S. L., Xu, M. L. et al., Simulated and experimental studies on identification of impact load with the transient statistical energy analysis method, *Mechanical Systems and Signal Processing*, **46**, 307–324, (2014). https://doi.org/10.1016/j.ymssp.2014.01.015

[16] Song, H. Y., Yu, K. P., Li, X. Y. et al., Analysis on dynamic response error in transient, *Ship Science and Technology*, **38**, (2016).

[17] Sui, F. S., Ichchou, M. N. and Jezequel, L., Prediction of vibroacoustic energy using a discretized transient local energy approach and comparison with TSEA, *Journal of Sound and Vibration*, **251**, 163–180, (2002). https://doi.org/10.1006/jsvi.2001.3786

[18] Sui, F. S., Ichchou, M. N. and Jezequel, L., Prediction of transient vibration envelopes using statistical energy analysis techniques, *Journal of Vibration and Acoustics*, **112**, 127–137, (1990). https://doi.org/10.1115/1.2930088

[19] Langley, R. S., Hawes, D. H. and Butlin, T. Y., A derivation of the transient statistical energy analysis equations with benchmark applications to plate systems, *Journal of Sound and Vibration*, **445**, 88–102, (2019). https://doi.org/10.1016/j.jsv.2019.01.002

[20] Langley, R. S., On the statistical mechanics of structural vibration, *Journal of Sound and Vibration*, **466**, 115034, (2020). https://doi.org/10.1016/j.jsv.2019.115034

[21] Tso, Y. K. and Hansen, C. H., The transmission of vibration through a coupled periodic structure, *Journal of Sound and Vibration*, **215**, 63-79, (1998). https://doi.org/10.1006/jsvi.1998.1608

[22] Robinson, M. and Hopkins, C., Prediction of maximum fast time-weighted sound pressure levels due to transient excitation from the rubber ball and human footsteps, *Building and Environment*, **94**, 810–820, (2015). https://doi.org/10.1016/j.buildenv.2015.06.013

[23] Hirakawa, S. and Hopkins, C., Experimental determination of transient structure-borne sound power from heavy impact sources on heavyweight floors with floating floors using an inverse form of transient statistical energy analysis, *Applied Acoustics*, **140**, 74–82, (2018). https://doi.org/10.1016/j.apacoust.2018.05.020

[24] Hopkins, C. and Robinson, M., Using transient and steady-state SEA to assess potential errors in the measurement of structure-borne sound power input from machinery on coupled reception plates, *Applied Acoustics*, **79**, 35–41, (2014). https://doi.org/10.1016/j.apacoust.2013.12.013

[25] Chen, Q., Fei, Q. G., Wu, S. Q. et al., An efficient transient analysis method for time-varying structures based on statistical energy analysis, *Mechanics Research Communications*, **91**, 93–99, (2018). https://doi.org/10.1016/j.mechrescom.2018.06.001

[26] Li, M. Q., *Research on the transient statistical energy method of high frequency shock environment of submarine structure*, Harbin Engineering University, (2018).

[27] Guo, J., *Research on characteristics of impact environment of stiffened double cylindrical shell*, Harbin Engineering University, (2008).

[28] Gong, S. W. and Khoo, B. C., Transient response of stiffened composite submersible hull to underwater explosion bubble, *Composite Structures*, **122**, 229–238, (2015). https://doi.org/10.1016/j.compstruct.2014.10.026

[29] Gong, S. W., Transient response of stiffened composite submersible hull to underwater shock and bubble, *Composite Structures*, **213**, 243–251, (2019). https://doi.org/10.1016/j.compstruct.2019.01.097

[30] Sykora, H. T., Kuske, R. and Yurchenko, D., Systematic matrix formulation for efficient computational path integration, *Computers and Structures*, **273**, 106896, (2022). https://doi.org/10.1016/j.compstruc.2022.106896

[31] Wehner, M. F. and Wolfer, W., Numerical evaluation of path-integral solutions to Fokker–Planck equations, *Physical Review A*, **27**, 2663, (1983). https://doi.org/10.1103/PhysRevA.27.2663

[32] Wehner, M. and Wolfer, W., Numerical evaluation of path-integral solutions to Fokker–Planck equations. II. Restricted stochastic processes, *Physical Review A*, **28**, 3003, (1983). https://doi.org/10.1103/PhysRevA.27.2663

[33] Wehner, M. and Wolfer, W., Numerical evaluation of path-integral solutions to Fokker–Planck equations. III. Time and functionally dependent coefficients, *Physical Review A*, **35**, 1795, (1987). https://doi.org/10.1103/PhysRevA.35.1795

[34] Johnson, E. A., Wojtkiewicz, S. F., Spencer, B. F. et al., Observations with regard to massively parallel computation for Monte Carlo simulation of stochastic dynamical systems, *International Journal of Non-Linear Mechanics*, **32**, 721–734, (1997). https://doi.org/10.1016/S0020-7462(96)00097-2

[35] Pinnington, R. J. and Lednik, D., Transient statistical energy analysis of an impulsively excited two oscillator system, *Journal of Sound and Vibration*, **189**, 249–264, (1996). https://doi.org/10.1006/jsvi.1996.0018

[36] Yao, D. Y. and Wang, Q. Z., *Principles and applications of statistical energy analysis*, Beijing Institute of Technology Press, Beijing, (1995).

[37] Zhang, Z. J., Wu, C., Pang, F. Z. et al., Research on test of ship typical structure component loss factor, *Transducer and Microsystem Technologies*, **34**, 30–32+36, (2015).

[38] Pang, F. Z., Li, H. C. and Peng, D. W., Transient vibration analysis of cylindrical shells with complex boundary conditions, *Journal of Harbin Engineering University*, **40**, 1238–1244, (2019).

[39] Robinson, M. and Hopkins, C., Prediction of maximum time-weighted sound and vibration levels using transient statistical energy analysis. Part 1: Theory and numerical implementation, *Acta Acustica united with Acustica*, **100**, 46–56, (2014). https://doi.org/10.3813/AAA.918685

[40] Guasch, O. and García, C., Numerical local time stepping solutions for transient statistical energy analysis, *Journal of Vibration and Acoustics*, **136**, 064502, (2014). https://doi.org/10.1115/1.4028454